Eur. Phys. J. A **3**, 159–164 (1998)

THE EUROPEAN PHYSICAL JOURNAL A

Light charged particle emission induced by neutrons with energies between 25 and 65 MeV on oxygen. II. Tritons and alpha-particles

S. Benck[1], I. Slypen[1], J.P. Meulders[1], V. Corcalciuc[2]

[1] Institut de Physique Nucléaire, Université Catholique de Louvain, Chemin du Cyclotron 2, B-1348 Louvain-la-Neuve, Belgium
[2] Institute for Atomic Physics, PO Box MG6, Bucharest, Romania

Received: 24 April 1998 / Revised version: 1 July 1998
Communicated by D. Schwalm

Abstract. Double-differential cross sections for fast neutron induced triton and alpha-particle production on oxygen, are reported at seven incident neutron energies between 30 and 65 MeV. Angular distributions were measured at laboratory angles between 20° and 160°. Energy-differential, angle-differential and total cross sections are reported. Experimental cross sections are compared with existing experimental data and with theoretical model calculations.

PACS. 25.40.-h Nucleon-induced reactions – 25.40.Hs Transfer reactions – 28.20.-v Neutron physics

1 Introduction

We report here experimental double-differential cross sections ($d^2\sigma/d\Omega dE$) and their angular distributions, measured at laboratory angles between 20° and 160° in steps of 10°, for triton and alpha-particle emission induced by fast neutrons on oxygen, at seven incident neutron energies: 34.5 ± 1.5, 37.5 ± 1.5, 41.0 ± 2.0, 45.0 ± 2.0, 49.0 ± 2.0, 53.5 ± 2.5 and 62.7 ± 2.0 MeV.

The reader is refereed to the preceding paper and references therein for most of the details of experimental set-up and data reduction procedures, therefore in Sec. 2, only particularities of data reduction procedures for tritons and alpha-particles are presented. Experimental results and comparison with other experimental data and theoretical calculations are presented in Sec. 3. Conclusions are covered in Sec. 4.

2 Data reduction

The protons and deuterons recoiling respectively from a 1 mm thick polypropylene and a 0.6 mm thick deuterated polypropylene target are used for the energy calibration. They are recorded at laboratory angles from 20° to 70° in steps of 10°, for each of the four telescopes. These measurements provide a reliable energy calibration for protons and deuterons. Previous experimental work on the light response of CsI crystals to the detection of a large variety of charged ejectiles, relates the crystal light response to the energy of the detected charged particle by a simple three free parameters analytical formula which is also dependent on the mass and charge (AZ^2) of the ejectile [1, 2]. Using this formula in a simultaneous fit to the proton and deuteron energy calibration points and a supplementary α-source point (at about 5.5 MeV), the three free parameters are determined. In this way a reliable energy calibration for tritons and alpha-particles, consistent with the energy calibration for protons and deuterons, was obtained. The errors on the three free parameters, induce errors in the energy calibration. The energy spectra for triton and alpha-particle production are reported here as histograms in steps of 3 MeV for the outgoing particle energies. As the measured cross sections are rather small, this choice of the energy step improves the statistics in the reported spectra.

Absolute cross sections are obtained by normalisation to our measured H(n,p) scattering cross sections, as explained in the preceding paper. Considering a minimum statistics of 10 counts in an ejectile energy bin (3 MeV for tritons and alpha-particles) and taking into account the thick target corrections (increasing as the detected ejectile energy decreases), a realistic estimation of the detection sensibility both for tritons and alpha-particles is of about 5×10^{-3} mb/MeVsr corresponding to 33% statistical error. This limit is valid for data obtained at 62.7 MeV (high energy peak). For incident neutron energies from the flat continuum of the incident neutron energy spectra, this limit becomes 5×10^{-2} mb/MeVsr due to the fact that there are about 10 times less neutrons in an low energy bin than in the main peak.

3 Experimental results and discussions

Previous experimental fast neutron induced triton and alpha-particle emission spectra have been reported by our group for carbon [3].

Final double-differential ($d^2\sigma/d\Omega dE$) cross-sections for triton and alpha-particle emission of the present work were obtained as follows: i) tritons: 62.7 MeV, which corresponds to the main peak of the incident neutron energy spectrum (full angular distribution, that is 13 angles in the range 20° to 160°), 53.5, 49.0, 45.0 and 41.0 MeV (7 forward angles starting with 20° lab) and ii) alpha-particles: same as for tritons plus 37.5 MeV (6 forward angles) and 34.5 MeV incident neutron energy (4 forward angles). In spite of our long measuring runs no significant statistics could be accumulated for other incident neutron energies or laboratory angles. Therefore, only superior limits can be inferred for these cross sections.

The reported alpha-particle spectra contain as well the ^{3}He ejectiles which could not be properly separated in the present experiment. Nevertheless their contribution is rather small and within the statistical errors of the alpha spectra [4].

The overall relative errors of the points in the spectra for 62.7 MeV (high energy peak in the neutron energy spectra) are about 17% for tritons and 33% for alpha-particles. For all the lower incident neutron energies the corresponding values are about 40% for tritons and 55% for alpha-particles. They include statistical errors and errors induced by thick target corrections.

For all the incident neutron energies, the uncertainty of the cross section absolute scale is 7–8%, given by errors in the measured reference H(n,p) cross sections, solid angle corrections, beam monitoring etc.

Low energy cuts in the spectra are 12 MeV both for tritons and alpha-particles. For alpha-particles they are due to thick target effects. The rather high value for tritons is mainly the result of the poor separation in the low energy part of the charged particle discrimination spectra.

Figures 1, 2 present double-differential cross sections at 20° lab vs incident neutron energy, for respectively tritons and alpha-particles. Filled dots indicate data of the present work in 3 MeV energy steps. The triangles are experimental data for neutron induced charged particle production on oxygen at 60.7 and 39.7 MeV [4]. The agreement of the two experimental data sets is good for both ejectiles. Theoretical calculations with the intranuclear cascade model (INCA) [5] are shown as histograms. At incident neutron energies 53.5, 45.0 and 37.5 MeV the shown histograms result as a linear interpolation of the calculated ones. For alpha-particles, the GNASH nuclear model code predictions [6] are indicated as continuous lines. The intranuclear cascade model underpredicts largely the measured cross sections for tritons. As most of the measured cross sections in Fig. 1 are rather low (0.1 to 0.3 mb/MeVsr) and comparable with the sensibilities on the cross section tables of [5], it might be that the statistics used in the Monte-Carlo simulation (INCA) is too poor. The alpha-particle experimental spectra are well described both by the INCA and GNASH calculations.

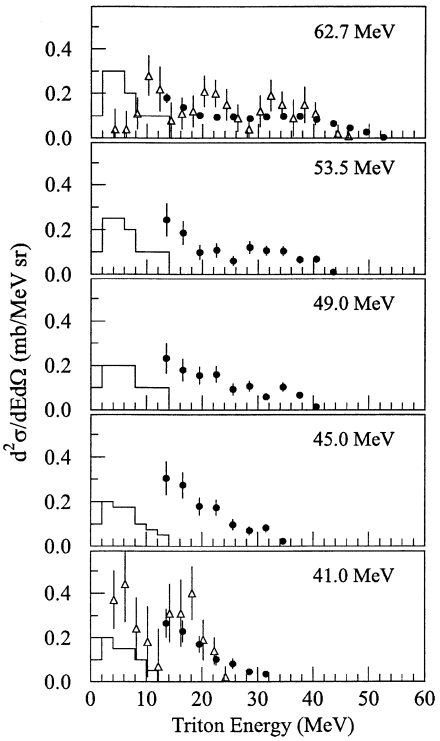

Fig. 1. Double-differential cross sections ($d^2\sigma/d\Omega dE$) for ^{16}O(n,tx) reactions at 20° lab, for the five indicated incident neutron energies. Filled dots represent data of this work in 3 MeV steps. Similar experimental data [4] are shown as triangles. Intranuclear cascade model calculations INCA [5] are presented as histograms

Energy spectra are presented, at several laboratory angles, respectively for tritons and alpha particles at 62.7 MeV incident neutron energy, in Figs. 3, 4. The stars indicate experimental data for respectively ^{16}O(p,^{3}Hex) and ^{16}O(p,αx) reactions [7]. All the other symbols are the same as in Figs. 1, 2. The three experimental data sets agree within the errors (rather large for those of [4]). The INCA calculations give cross sections only for very low triton energies (Fig. 3), at the limit of the experimental low energy cuts. In the alpha-particles case, INCA calculations underpredict the high energy part of the spectra, specially at backward angles. The GNASH nuclear model code gives a good description of the energy spectra in Fig. 4.

Figure 5 presents double-differential cross sections at 10° lab, for tritons and alpha-particles in 3 MeV steps (filled dots) as result of the extrapolation procedure explained in the preceding article, compared to experimental data from proton induced reactions on oxygen at 61.5 MeV incident energy [7] (stars). The agreement of the two experimental data sets gives confidence in our extrapolation procedure at very forward angles. GNASH calculations (continuous lines) describe rather well the alpha-particle spectra. The intranuclear cascade model INCA calculations (histograms) predict for tritons much less cross section than obtained by the extrapolation and for alpha-particles overestimate the high energy part of the spectra.

The angle integration of the double-differential cross section angular distributions, provides the energy-

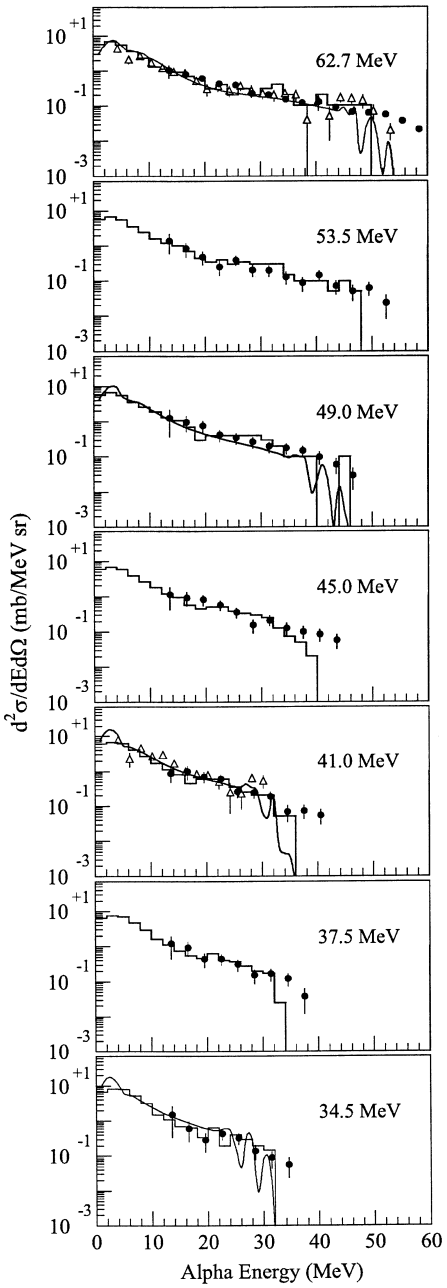

Fig. 2. Same as in Fig. 1 for the case of ^{16}O(n,αx) reactions but for 7 incident neutron energies. Continuous lines indicate GNASH calculations [6]

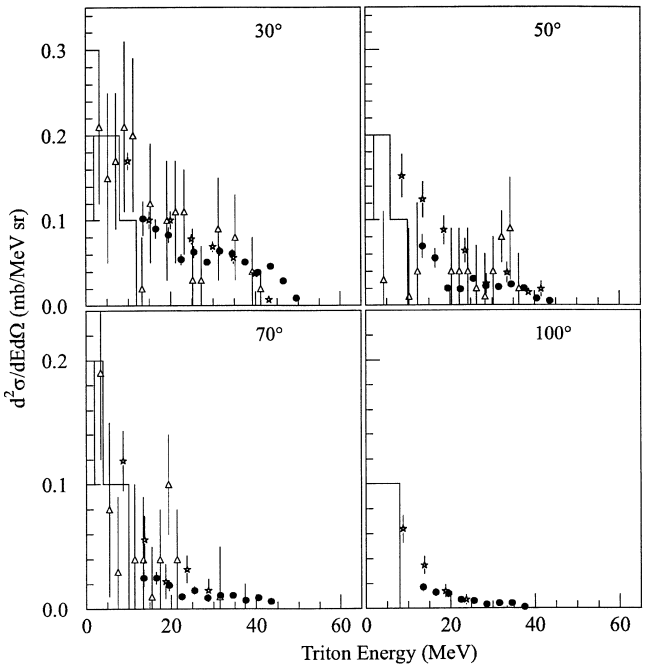

Fig. 3. Measured double-differential cross-sections at four laboratory angles (filled dots in steps of 3 MeV) for ^{16}O(n,tx) reactions at 62.7 MeV incident neutron energy. Corresponding experimental data [4] are shown as triangles. Our 30°, 50° and 70° spectra are compared to respectively 35°, 45° and 65° data of [4]. The stars indicate results for ^{16}O(p,^{3}Hex) reactions at 61.5 MeV [7]. The histograms are theoretical INCA predictions [5]

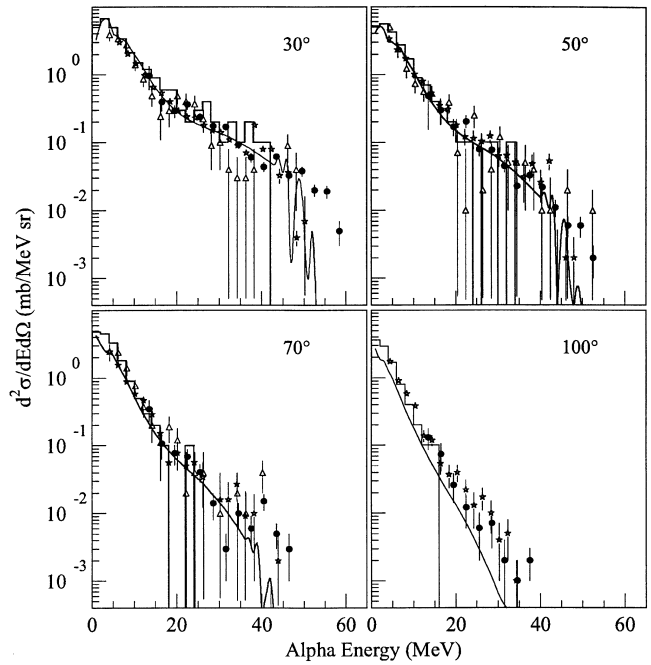

Fig. 4. Same as in Fig. 3 for the case of ^{16}O(n,αx) reactions. Continuous lines indicate GNASH calculations [6]

differential cross sections (dσ/dE). Experimental energy-differential cross sections are shown for tritons at 5 incident neutron energies in Fig. 6 and for alpha-particles at 7 incident neutron energies in Fig. 7. For more clarity, only alpha-particle energies higher than 10 MeV are shown in Fig. 7. For 62.7 MeV incident neutron energy, reliable energy-differential spectra for tritons and alpha-particles are obtained, as the complete angular distributions have been measured. For lower incident neutron energies (corresponding to the continuum of the incident neutron energy spectrum) the measured angular distributions are incomplete due to the lack of accumulated statistics at angles higher than 80° lab. Therefore, the extrapolation procedures are questionable. Nevertheless, as most of the cross section is concentrated at forward angles it is reasonable

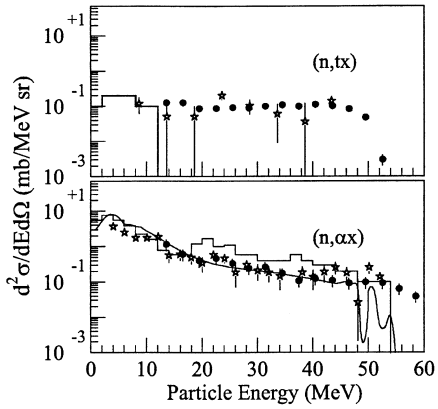

Fig. 5. Extrapolated double-differential cross sections at 10° lab (filled dots in steps of 3 MeV) for ^{16}O(n,tx) and ^{16}O(n,αx) reactions at 62.7 MeV incident neutron energy. The stars indicate experimental measurements at 61.5 MeV for respectively ^{16}O(p,^{3}Hex) and ^{16}O(p,αx) reactions [7]. The histograms are theoretical INCA predictions [5] and continuous lines indicate GNASH calculations [6]

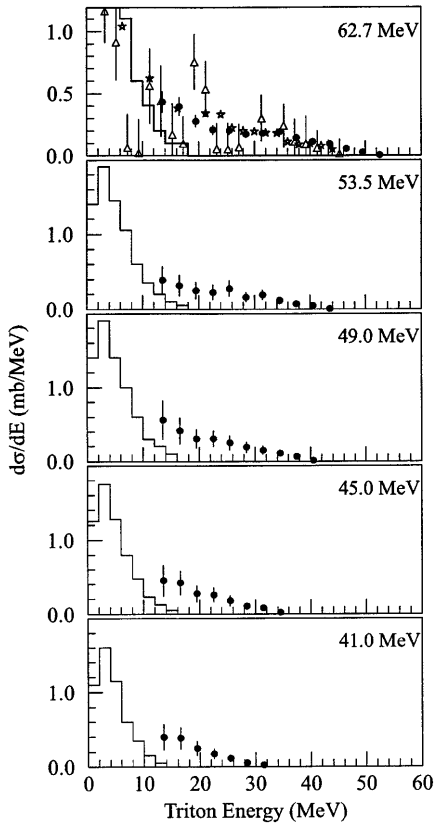

Fig. 6. Energy-differential cross sections (in steps of 3 MeV) for ^{16}O(n,tx) reactions at the indicated five incident neutron energies (filled dots). Triangles represent corresponding experimental data [4] and stars those for ^{16}O(p,^{3}Hex) reactions [7]. INCA theoretical predictions [5] are shown as continuous lines

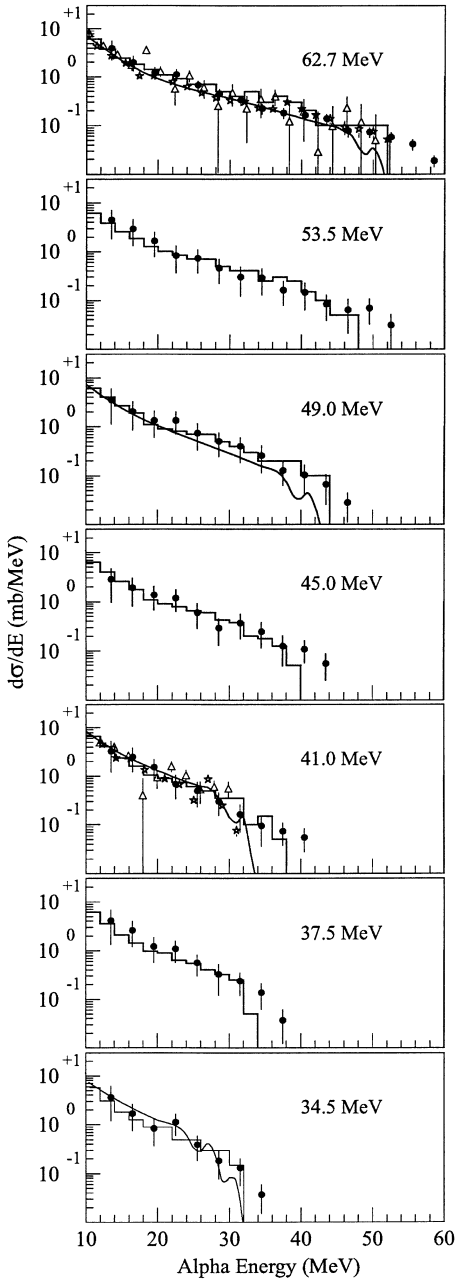

Fig. 7. Same as in Fig. 6 for the case of ^{16}O(n,αx) reactions for seven incident neutron energies. Continuous lines indicate GNASH calculations [6]

to suppose that the obtained energy-differential spectra in these cases are rather close to the reality. A convenient check was to calculate an upper and a lower limit for the energy-differential cross sections in Figs. 6, 7, at incident neutron energies lower than 62.7 MeV, by respectively considering the 90° extrapolated cross sections as a constant for all angles higher than 90° lab or considering a zero value cross sections for these angles. These two limits are within the errors of the energy-differential cross sections in Figs. 6, 7. In all the shown energy-differential cross sections, contributions from extrapolated double-differential spectra (as explained in the previous paper) are included as well. For both tritons and alpha-particles, the experimental data for neutron [4] (triangles) and for

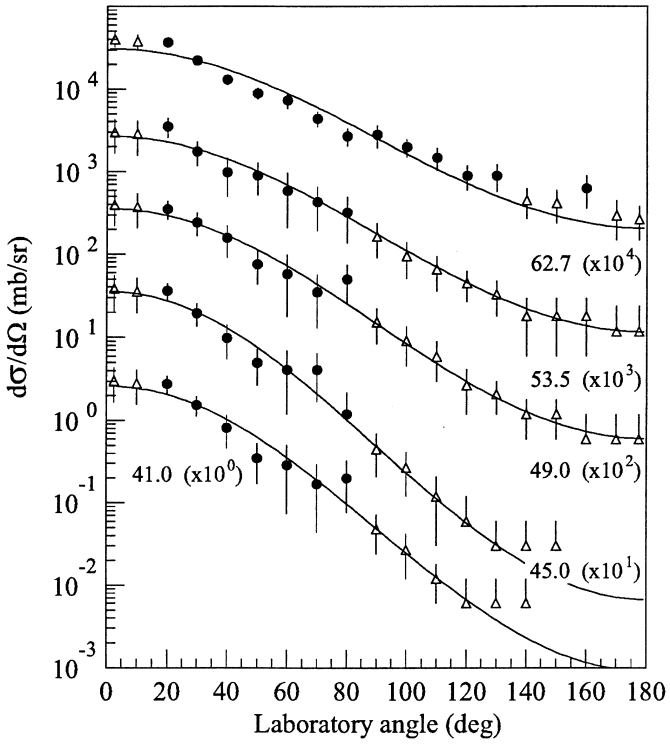

Fig. 8. Experimental angle-differential cross sections for triton emission at the indicated five incident neutron energies (filled dots). The experimental low energy thresholds are 12 MeV. The triangles represent extrapolation of the experimental data. In parenthesis are scale factors as decades. The lines serve to guide the eye

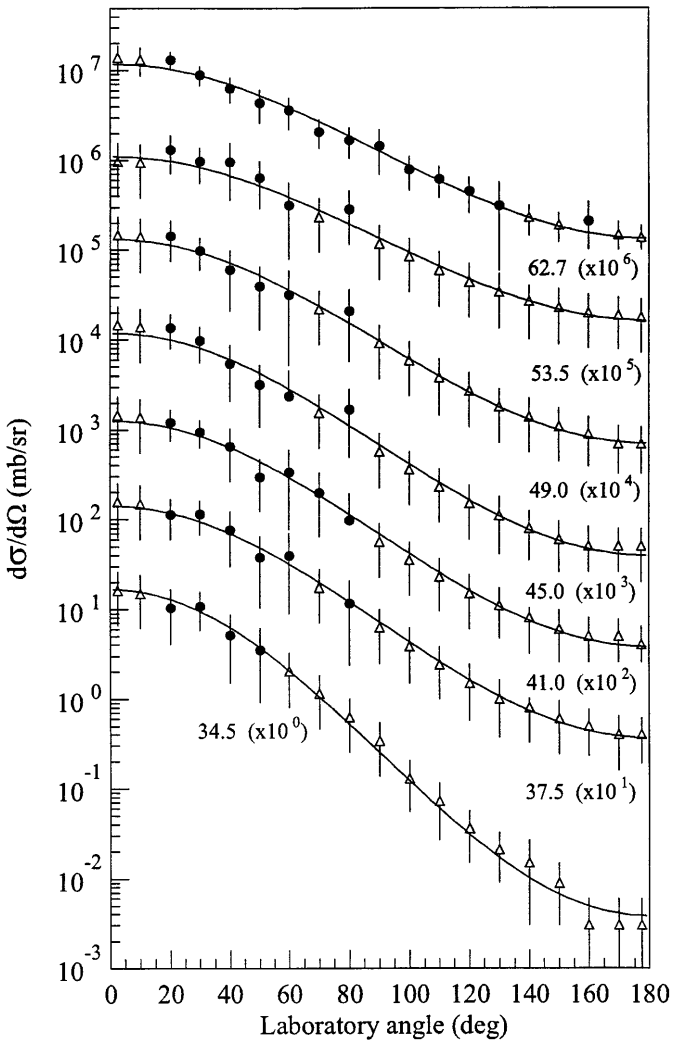

Fig. 9. Same as in Fig. 8 for the case of alpha-particles at 7 incident neutron energies. The experimental low energy thresholds are 12 MeV. In parenthesis are scale factors as decades

proton induced [7] reactions (stars) on oxygen (for 61.5 and 39.0 MeV incident proton energy) are indicated. For tritons in Fig. 6, data are for (p,^{3}Hex) reactions [7]. The agreement of the three experimental data sets is good. The INCA calculations [5] (histograms) strongly underpredict the experimental cross sections for tritons. For alpha-particles, both theoretical calculations, INCA and GNASH [6], describe very well the experimental data.

Angle-differential cross sections ($d\sigma/d\Omega$) are presented in Fig. 8 for tritons and in Fig. 9 for alpha-particles at the indicated incident neutron energies. Filled dots represent the result of the energy integration of the double-differential cross sections for the laboratory angles where statistics were accumulated. Triangles result from the energy integration of extrapolated double-differential cross sections. Continuous lines in Figs. 8, 9 are to guide the eye. For clarity in Figs. 8, 9 the inferior error bars are not represented for some of the points.

Table 1 and Table 2 give total cross sections for respectively triton and alpha-particle emission, resulting from the integration of the energy-differential cross sections in Figs. 6, 7, together with the theoretical predictions based on INCA model [5] and GNASH model code calculations [6] (only in Table 2). For both theories, predicted cross sections under and above the experimental low energy cuts in the experimental spectra are indicated. Compared with the theory, the experimental results for alpha-particles in Table 2 indicate that only 7%–15% of the total cross section was measured in the experiment, the rest being concentrated at ejectile energies lower than 12 MeV.

Table 1. Experimentally measured total cross-sections (mb) of this work, for triton emission induced by fast neutrons on oxygen. Theoretical values from INCA [5] are given for above and, in parenthesis, below the experimental low energy threshold (12 MeV). Some of the indicated theoretical values result from a linear interpolation of the calculated ones

E_n (MeV)	σ(n,tx) (mb) (this work)	σ(n,tx) (mb) [5]
62.7 ± 2.0	7.4 ± 1.2	1.1 (13.8)
53.5 ± 2.5	6.1 ± 2.6	1.0 (13.5)
49.0 ± 2.0	7.0 ± 2.9	0.9 (13.2)
45.0 ± 2.0	5.4 ± 2.2	0.7 (11.6)
41.0 ± 2.0	4.1 ± 1.7	0.5 (9.9)

Table 2. Experimentally measured total cross-sections (mb) of this work, for alpha-particle emission induced by fast neutrons on oxygen. Theoretical values from INCA [5] and GNASH [6] are given for above and, in parenthesis, below the experimental low energy threshold (12 MeV). Some of the indicated theoretical values result from a linear interpolation of the calculated ones

E_n (MeV)	σ(n,αx) (mb) (this work)	σ(n,αx) (mb) [5]	σ(n,αx) (mb) [6]
62.7 ± 2.0	32.3 ± 10.9	31.5 (332.2)	25.4 (223.6)
53.5 ± 2.5	36.8 ± 20.8	30.5 (332.3)	25.2 (244.3)
49.0 ± 2.0	31.5 ± 18.6	29.4 (332.4)	25.0 (265.0)
45.0 ± 2.0	27.1 ± 15.8	27.5 (345.4)	27.0 (314.0)
41.0 ± 2.0	27.6 ± 15.3	25.5 (358.4)	29.0 (363.0)
37.5 ± 1.5	30.9 ± 18.2	22.5 (380.9)	27.8 (380.0)
34.5 ± 1.5	24.1 ± 14.5	19.5 (403.4)	26.5 (397.5)

4 Conclusions

Triton and alpha-particle emission energy spectra ($d^2\sigma/d\Omega dE$) resulting from the interaction of fast neutrons on oxygen, are reported at several incident energies between 30 and 65 MeV. Angular distributions were measured at laboratory angles between 20° and 160° (in steps of 10°).

Complete angular distributions of the energy spectra are obtained both for tritons and alpha-particles for 62.7 MeV incident neutron energy. For other 4 incident neutron energies (53.5, 49.0, 45.0 and 41.0 MeV) in the triton case and 6 incident neutron energies (53.5, 49.0, 45.0, 41.0, 37.5 and 34.5 MeV) in the alpha-particle case, energy spectra are reported only at forward angles. Due to the low statistics accumulated, only superior limits can be established for the double-differential cross sections at higher angles for the above mentioned incident neutron energies.

The present data are in fair agreement with previous measurements on neutron induced charged particle production on oxygen [4] and in good agreement with experimental results from proton induced reactions on oxygen [7].

Experimental data are compared with intranuclear cascade model calculations INCA [5]. The triton emission cross sections are strongly underestimated while the alpha-particle spectra are well reproduced at forward angles, both for the shape of the spectra and for the absolute magnitude of the cross-sections. Nevertheless, the model predicts less high energy alpha-particles than experimentally observed at backward angles. The GNASH predictions [6] are in very good agreement with the experimental alpha-particle spectra.

Similar conclusions are valid for the deduced energy-differential ($d\sigma/dE$) spectra.

Angle-differential ($d\sigma/d\Omega$) and total cross sections (σ_T), as resulting from our experiment are also presented.

Complete double-differential production cross sections and their angular distributions may be obtained from Mrs. S. Benck.

We would like to thank the Louvain-la-Neuve Cyclotron staff for permanent assistance and quality of the beam. We acknowledge support of the Institut Interuniversitaire des Sciences Nucleaires, Belgium and partly the European Economic Community (contract FI3P-93-0084-BE). Thanks are due to M. B. Chadwick for providing detailed numerical values as result of [6].

References

1. D. Horn, C. G. Ball, A. Galindo-Uribarri, E. Hagberg, R. B. Walker, R. Laforest, and J. Pouliot, Nucl. Instrum. Methods Phys. Res. Sect. A**321**, 273 (1992)
2. F. Bernachi, B. Chambon, B. Cheynis, D. Drain, C. Pastor, D. Seghier, K. Zaid, A. Giorni, D. Heuer, A. Leres, C. Morand, P. Stassi and J. B. Viano, Nucl. Instrum. Methods A**281**, 137 (1989)
3. I. Slypen, V. Corcalciuc, J. P. Meulders and M. Chadwick, Phys. Rev. C**53** 1309 (1996)
4. T. S. Subramanian, J. L. Romero, F. P. Brady, D. H. Fitzgerald, R. Garett, G. A. Needham, J.L. Ullmann, J. W. Watson, C. I. Zanelli, D. J. Brenner and R. E. Prael, Phys. Rev. C**34**, 1580 (1986); J. L. Romero, private communication (1994)
5. D. J. Brenner and R. E. Prael, Atomic and Nucl. Data Tables **41**, 71 (1989)
6. M. B. Chadwick, P. G. Young, Nucl. Sci. Eng. **123**, 1 (1996); M. B. Chadwick, Private communication to S. Benck
7. F. E. Bertrand and R. W. Peelle, Phys. Rev. C**8**, 1045 (1973); F. E. Bertrand and R. W. Peelle, Oak Ridge Report, ORNL-4799 (1973)